ORIGINAL PAPER

A spatiotemporal analysis of droughts and the influence of North Atlantic Oscillation in the Iberian Peninsula based on MODIS imagery

Stefan Mühlbauer[1] · Ana Cristina Costa[1] ·
Mário Caetano[1]

Abstract Drought is among the least understood hazards and requires particular notice in the context of climate change. While the Mediterranean climate is by itself prone to droughts, a rise of temperatures and alteration of rainfall patterns already render the southern parts of continental Portugal and Spain highly susceptible to desertification. Precipitation in the Iberian Peninsula is mainly controlled by the large-scale mode of North Atlantic Oscillation (NAO) and is distributed with elevated variability over the cold months. Most drought studies of this region rely on meteorological data or apply information on vegetation dynamics, such as the Normalised Differenced Vegetation Index (NDVI), to indirectly investigate droughts. This paper evaluates the influence of the NAO winter index on the spatiotemporal occurrence of droughts in the Iberian Peninsula during the spring and summer seasons (March to August) for the years 2001–2005, 2007 and 2010. We applied the Vegetation Temperature Condition Index (VTCI) to identify local droughts. VTCI is a remote sensing drought index developed for reflecting soil moisture conditions in agricultural areas and combines information on land surface temperature (LST) and NDVI. As such, VTCI overcomes the shortcomings of NDVI in terms of drought monitoring. We derived biweekly information on LST and NDVI from MODIS/Terra and produced VTCI–NAO correlation maps at a confidence level of at least 90 % based on the VTCI time series. The results reflect a typical Mediterranean pattern in most parts of Iberia that is highly influenced by relief. Spring seasons are marked by great variability of precipitation, while summers persistently become dry, particularly in the south. NAO exerts its greatest influence in April and June, clearly delineating high correlation areas in the northwest and southeast with reverse patterns between the spring and early summer months. Due to the impact on water availability, the spring months are important for plant growth. At the same time, agricultural lands were found with types of land cover less resilient to droughts. The knowledge acquired in studies like the one reported here is therefore likely to be used in drought warning models for agriculture in spring.

✉ Stefan Mühlbauer
stefan.muehlb@yahoo.de

[1] ISEGI, Universidade Nova de Lisboa, Campus de Campolide,
1070-312 Lisboa, Portugal

1 Introduction

Drought is a natural disaster that can exert serious harm on the society, the environment and the economy (Ji and Peters 2003; Santos et al. 2010). About half of the terrestrial surfaces on earth are located in areas prone to drought, and more dramatically, almost all major agricultural lands extend in such regions (USDA 1994). Of all environmental disasters within the twentieth century, droughts entailed the greatest detrimental impact (Mishra and Singh 2010). Although mainly driven by precipitation deficits, drought is sensitive to preconditions such as land cover/use, type of soil, elevation and human-induced activities, when an increased demand of water supply from agriculture, industry and tourism may result in water scarcity (Pereira and Paulo 2004; Paredes et al. 2006). Hence, drought lacks a universally accepted definition. The most general characterisation is perhaps the one that considers the phenomenon as a recurring natural disaster caused by a temporary deficit in water supply. Drought may reduce soil moisture, streams and groundwater resources, deteriorate

water quality, damage vegetation cover, degrade ecosystems and agricultural lands and also affect human beings (Mishra and Singh 2010; Rojas et al. 2011). This leads to the identification of five types of drought: meteorological, hydrological, agricultural, ecological and socioeconomic.

The remote sensing drought index applied in this paper corresponds to soil moisture conditions and indirectly reflects precipitation patterns. As such, it describes the hydrological or agricultural type of water scarcity (Choi et al. 2013). Nevertheless, we consider drought a natural hazard driven by atmospheric factors from synoptic to large-scale modes. The predictability of drought among atmospheric disasters is lowest due to its sensitivity to a number of environmental influences (Mishra and Singh 2010). The Iberian Peninsula regularly suffers water deficits that cause serious damage particularly to non-irrigated agriculture during drought years, degrading the environment and enhancing soil erosion (Vicente-Serrano 2006; Costa and Soares 2012). Since climate change and the rise of surface temperature have been recognised as a major threat of the twenty-first century, the drought issue belongs to one of the most explosive environmental topics for the research community, the public worldwide as well as in Portugal and Spain (Mishra and Singh 2010; Costa and Soares 2012).

The Iberian climate is strongly influenced by the atmospheric circulation pattern of the North Atlantic Oscillation (NAO). The NAO index compares the occurrence of high barometric pressure zones around the Azores and low barometric pressure systems in the North Atlantic (Iceland) and is expressed as the difference of normalised sea level pressure between both regions. The NAO determines the climatic variability in the North Atlantic throughout the year where it controls the direction and intensity of storm tracking paths, which is decisive for the precipitation regime in Iberia, because low pressure systems from the Atlantic account for the major source of winter rainfall (Hurrell 1995; Goodess and Jones 2002; Trigo et al. 2002, 2004; Vicente-Serrano and Trigo 2011). The impact of NAO on vegetation dynamics and phenology in Europe and the Mediterranean Basin has been studied several times (e.g. Trigo et al. 2002; Gouveia and Trigo 2011). Vicente-Serrano and Heredia-Laclaustra (2004) detected a positive trend of vegetation production given as the sum of Normalised Differenced Vegetation Index (NDVI) from 1982–2000 in the north and a negative trend in the south of Iberia, where at the same time, the NAO influence was found higher (Rodríguez-Puebla et al. 1998; Gouveia et al. 2008). This observation also coincides with the findings of Martín-Vide and Fernández (2001), who describes a major influence of NAO on precipitation in the southwest of Iberia during the winter months, while the other regions rely on other teleconnection patterns such as the Polar Pattern or the Scandinavian Pattern (Rodríguez-Puebla et al. 1998). The influence of NAO also extends to other parts of Europe. In their correlation analysis between NAO and vegetation greenness (NDVI), Gouveia et al. (2008) demonstrated that in Iberia, water accessibility from NAO-induced precipitation highly impacts vegetation growth in spring, while in northeast Europe, the influence of NAO on winter temperature is more decisive for a rapid start into the vegetation period. NAO is therefore the major large-scale mode that controls winter precipitation and impacts NDVI trends particularly in the northwest, south and southwest of Iberia.

Traditional drought monitoring methods rely on meteorological or hydrological data that are collected at single sampling stations (Santos et al. 2009; Caccamo et al. 2011). The majority of drought studies for the western Mediterranean applies such information (e.g. Trigo et al. 2002; Vicente-Serrano 2006; Costa and Soares 2009, 2012; Santos et al. 2010; Gouveia and Trigo 2011; Martins et al. 2012). The area-wide estimation of punctual accessible drought values is accomplished by spatial interpolation, by geostatistical interpolation, for example, and is susceptible to uncertainties especially over climatically and topographically complex terrain (Rhee et al. 2010; Caccamo et al. 2011). Remote sensing data that cover area-wide terrestrial surfaces over an extended period have therefore acquired interest in drought assessment (Martín-Vide and Fernández 2001; Vicente-Serrano and Heredia-Laclaustra 2004; Bayarjargal et al. 2006). In areas with a low density of sample stations, they may be the only source of available information (Caccamo et al. 2011).

Among remote sensing indices, the NDVI is the most widely used for drought analysis. NDVI was introduced by Rouse et al. (1974) to catch the difference between red and near-infrared solar radiation emitted by green plants and reflects the condition of vegetation and its dynamics over the year (Vicente-Serrano and Heredia-Laclaustra 2004). NDVI is correlated to precipitation with a time gap of 1–2 months (Wang et al. 2001) or 3 months as reported by Ji and Peters (2003) depending on the kind of vegetation and soil type. The latter authors argued that NDVI is a good indicator of vegetation moisture conditions and can be used as indirect information for drought monitoring if related to a long-term NDVI series. NDVI indeed became part of numerous remote sensing drought indices, such as the Vegetation Condition Index (VCI; Kogan 1990, 1995), the Normalised Difference Water Index (NDWI; Gao 1996), the Vegetation Temperature Index (VTI; Kogan 1997), the Vegetation Health Index (VHI; Kogan 2000) and the Temperature Vegetation Dryness Index (TVDI; Sandholt et al. 2002) to mention some of them and was successfully used for identifying droughts on regional or local scales (Peters et al. 1993; Nicholson et al. 1998; Gonzalez-Alonso et al. 2000; Liu and Negron-Juarez 2001; Salinas-Zavala et al. 2002; Ji and Peters 2003). However, NDVI has shortcomings that may cause problems when solely used for drought monitoring. The mentioned deficits are its lagged time response to cumulative rainfall (Davenport and

Nicholson 1993; Wang et al. 2001; Gouveia et al. 2008), its sensitivity towards environmental preconditions, such as the type of soil, climate and vegetation (Singh et al. 2003; Vicente-Serrano 2007), the fact that the NDVI signal saturates before the full biomass is reached (Carlson et al. 1990; Carlson and Ripley 1997) and that the relationships among vegetation parameters are often non-linear (Choudhury et al. 1994; Vicente-Serrano and Heredia-Laclaustra 2004). In accordance to this discussion, a number of authors suggested the use of land surface temperature (LST) as a second variable for a more complex analysis as the drought related one (Kogan 1995; Park et al. 2004; Wan et al. 2004; Ghulam et al. 2007; Rhee et al. 2010; Wu et al. 2012; Lazzarini et al. 2013). LST is a parameter of the energy state on the earth's surface (Wan et al. 2004) and serves as an indicator for evapotranspiration, soil moisture and vegetation water stress (Karnieli et al. 2010). Practically, satellite-derived LST measures the temperature of the ground's skin over bare soil surfaces, of the vegetation canopy surface over densely vegetated areas and a mixture of all over sparsely vegetated terrain (Parida et al. 2008). LST can grow rapidly with increasing water stress due to changes in vegetation condition, vegetation cover and soil moisture. The physical fact that leaf surface temperature of green plants increases during dry conditions explains why LST raises slightly before vegetation cover decreases (Wan et al. 2004) and justifies its use for drought monitoring. LST was used, together with NDVI, in some of above stated drought indices. The LST–NDVI relationship was investigated several times in terms of vegetation cover, burnt areas, soil moisture, drought and climate change (Dall'Olmo and Karnieli 2002; Sandholt et al. 2002; Karnieli and Dall'Olmo 2003; Wan et al. 2004; Jang et al. 2006; Julien et al. 2006; Stisen et al. 2007). A strong negative correlation between LST and NDVI was revealed, and in the scatter plot, the LST–NDVI slope was found to become steeper under dry conditions (Nemani et al. 1993; Prihodko and Goward 1997; Goward et al. 2002). Karnieli et al. (2010) found that in mid and low latitudes of North America, solar radiation is the principal factor driving the LST–NDVI relationship, which affirms LST as a useful variable for drought monitoring.

The Vegetation Temperature Condition Index (VTCI) has been proposed for examining agricultural droughts (Wang et al. 2001; Wan et al. 2004). The VTCI approach is based on the theory that LST–NDVI space creates a triangle (Moran et al. 1994; Gillies et al. 1997; Wan et al. 2004). VTCI combines the variables in a more complex way than the ratio LST–NDVI, which better adapts to the needs of investigating such a complex phenomenon as drought in large regions with many land cover/use characteristics and high climatic variability. Moreover, it overcomes the disadvantages of NDVI, which faces a lagged vegetation response to droughts and makes it less suitable for real-time drought monitoring. Wang et al. (2001) evidenced that on a regional scale (144.1×

309.1 km^2), the VTCI reflects the simulated soil moisture content. Wan et al. (2004) showed in their study for the Great Plains (1001×853 km^2) that VTCI is related to not only recent rainfall but also cumulative rainfalls and enhances real-time drought monitoring.

The study at hand intends to complement the drought monitoring initiatives on the Iberian Peninsula (Pereira and Paulo 2004; Vicente-Serrano and Heredia-Laclaustra 2004; Vicente-Serrano 2006, 2007; Santos et al. 2007, 2010; Costa and Soares 2009, 2012; Gouveia et al. 2009; Gouveia and Trigo 2011; Costa et al. 2012; Martins et al. 2012; Paolo et al. 2012). We chose the VTCI for spatial and temporal identification of droughts, which so far was never applied for a drought analysis in this region. It directly retrieves soil moisture conditions while taking advantage of compound information on NDVI and LST. Also, until now, the VTCI was only applied for examining droughts in agricultural-dominated areas, but accommodating land classes ranging from arid to alpine environments the Iberian Peninsula comprises far more than low vegetation cover. We concentrated on the recent decade and chose the years 2001 to 2005. Because of the distinct positive (negative) NAO winter index in 2007 (2010), we added the mentioned years to the time series. Two VTCI maps per month were produced at time intervals of 16 days from March to August for all years. Hence, a detailed seasonal analysis was preferred over a longer inter-annual assessment. An object of further interest was the influence of NAO winter index on spatiotemporal drought occurrences in the Iberian Peninsula during spring and summer. The study aspires to the development of a local drought warning system for agriculture based on NAO.

2 Study area

The analysed territory comprises continental Portugal and Spain and constitutes a peninsula of about 580,000 km^2 situated in the most south-western edge of Europe. We included the Balearic Islands, which appeared in the clipped detail and manifested matching climatic conditions regarding the mainland (Fig. 1). The climate is characterised by an Atlantic fraction in the north and northwest and a Mediterranean section in major parts of the Iberian Peninsula. Iberian weather is influenced by elements of both subtropical and temperate climate. The circulation regime in winter is particularly affected by the westerlies, while the Azores anticyclone controls the weather scheme during the summer months and results in highly seasonal climatic behaviour (Paredes et al. 2006). Rainfall is greatly dependent on large-scale atmospheric variations (NAO) in the North Atlantic (Santos et al. 2010) and is mainly distributed over the winter months with peaks between December and February, when transient lows are steered along the tracks of the polar-front jet and the mid-latitude
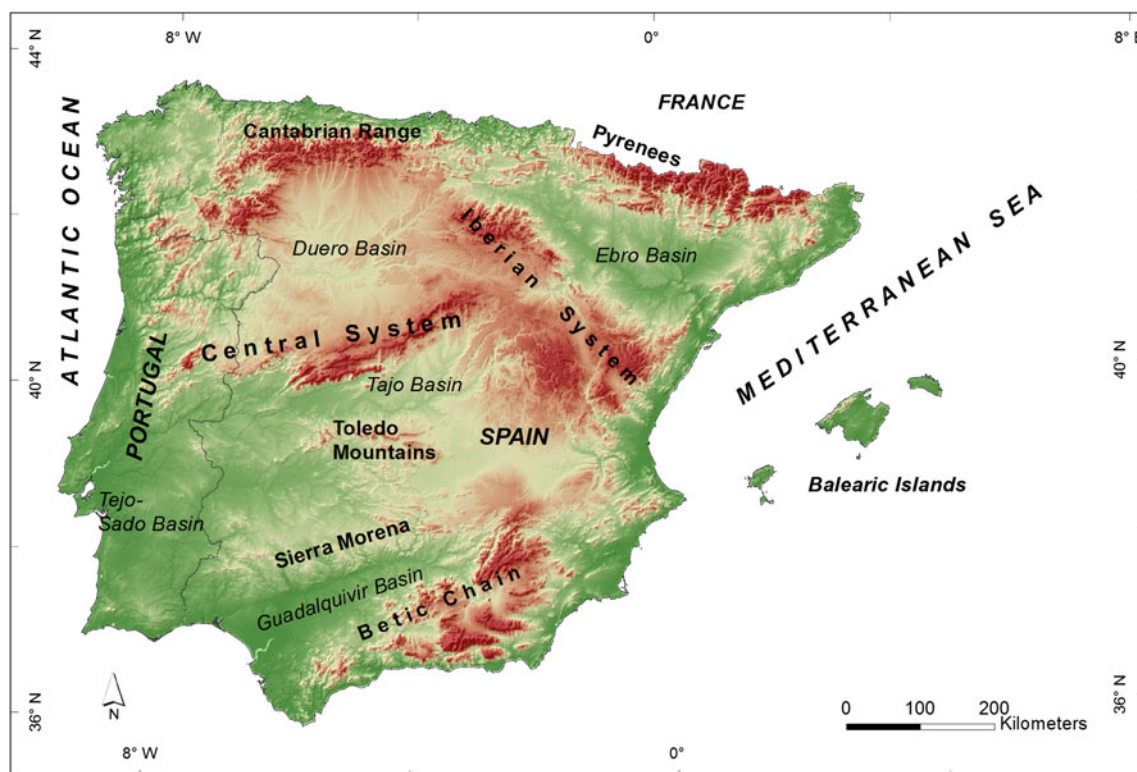
Fig. 1 Study area with boundaries and relief showing the most important mountain ranges (*brown*) and flat basins (*green*)

cyclonic ridge hits its southernmost position (Paredes et al. 2006; Costa and Soares 2012). A strong (weak) differentiation between a subtropical anticyclone and polar cyclone in the North Atlantic region determines dry (wet) years (Santos et al. 2009). Together with seasonal character, precipitations in the Iberian Peninsula are marked by a large spatiotemporal variability (Trigo et al. 2004; Vicente-Serrano 2006; Paredes et al. 2006; Costa and Soares 2012). Dry and wet years occur with some frequency resulting in a complex pattern of droughts that is characteristic for areas of climatic transition (Rodríguez-Puebla et al. 1998; Paredes et al. 2006). Accordingly, the Iberian Peninsula is highly sensitive to variations in precipitation and is prone to droughts (Trigo et al. 2004; Paredes et al. 2006; Vicente-Serrano 2006). Annual rainfall figures for the territory reflect its spatial variability and encompass averages of more than 1400 mm in Galicia (in the northwest) to less than 400 mm in the south and southeast of the peninsula (AEMET 2012). Relief and the land mass itself are important factors in local weather manifestation, because they direct air masses: major mountain ranges block precipitation and produce enhanced rainfall in windward areas, while sheltered zones receive much less precipitation. Relief impact explains the dry conditions of many basin situations.

Human activity over a long period (fire, pasturing, agriculture, forest plantations etc.) determines the manifestation of land cover in the Iberian Peninsula today. Natural vegetation

types are scarce. Nevertheless, the climatic diversity, relief, a low population density compared to European context and a loss of agricultural land in the last three decades all engender high environmental diversity (Lobo et al. 1997). The vegetation is characterised by an Atlantic region (deciduous vegetation) in the north and northwest as well as a Mediterranean region (sclerophyllous vegetation) in the south, east and centre of the Iberian Peninsula. Orographic plant communities complement the vegetation in areas of higher elevation.

3 Data and preprocessing

3.1 Satellite products

We used MODIS/Terra land surface products to acquire information on LST and NDVI for the spring and summer seasons of 2001–2005. The years 2007 and 2010 were added for their distinctive positive and negative NAO winter index (Table 1). The spring season is defined as March, April and May; June, July and August represent summer. MOD11A2 (LST) and MOD13A2 (NDVI) were acquired at the Land Process Distribution Active Archive Centre (LP DAAC). Both are globally available level-3 products at a spatial resolution of 1 km². VTCI maps were produced at 16-day intervals according to the availability of the MOD13A2 product starting in March at the day of the year (DOY) 065. To simplify, we

Table 1 NAO winter index (Gibraltar and Reykjavik) for the years 2001–2005, 2007 and 2010 (average values from Dec, Jan, Feb and Mar)

NAO winter index	
2000/1	−0.50
2001/2	+0.79
2002/3	+0.40
2003/4	−0.20
2004/5	−0.11
2006/7	+1.83
2009/10	−2.54

named the observation dates Mar 1, Mar 2, Apr 1, …, Aug 2. The MOD11A2 8-day product was adjusted to the intervals of NDVI. Four MODIS tiles cover the Iberian Peninsula. Accordingly, we downloaded 336 NDVI and 640 LST tiles (23 observation dates per year for LST; DOY169 in 2001 was not accessible). We projected and decoded the images corresponding to the MODIS Users' Guideline (Wan 2007; Solano et al. 2010), mosaicked and clipped them. We obtained the shapefiles from the global administrative area database (www.gadm.org). We also excluded all pixels of less than average quality, clouds, cloud shadows and heavy aerosols according to the quality flags of the MODIS Users' Guideline (Wan 2007; Solano et al. 2010). Negative NDVI pixels were omitted because they represented water, snow or ice. Excluded pixels appear white (*NoData*) and accumulate in early spring months due to enhanced cloud cover. We finally obtained 12 VTCI maps for each year. The VTCI map for Jun 1 2001 is missing because the source data was not accessible; thus, a total of 83 VTCI maps was produced.

3.2 Digital elevation model and land cover map

A digital elevation model was acquired at the Earth Science Data Interface of the Global Land Cover Facility from http://glcfapp.glcf.umd.edu:8080/esdi/esdi_index.jsp. It was downloaded as a SRTM30 GTOPO30 mosaic. This is a near-global digital elevation model with a resolution of 30 arc seconds. For the land cover analysis, we used the CORINE land cover map 2006 (CLC2006) from the European Environmental Agency (EEA 2013). We reclassified the map and obtained 14 of originally 44 classes pursuant to the third level description. All maps were transformed to the prevalent projected coordinate system in Spain to UTM30 N with datum WGS84.

3.3 NAO

The NAO is defined as the normalised pressure difference between a station on the Azores (Ponta Delgada) and one in Iceland (Reykjavik). An extended version using a station in the southwest of the Iberian Peninsula proved to be useful for the winter half of the year (Hurrell 1995). The NAO winter index is computed as the mean NAO value for the months of December, January, February and March (Osborn et al. 1999). The Climatic Research Unit (CRU) at the University of East Anglia is a major institution for NAO research and stores the index values from 1821 to 2000 (http://www.cru.uea.ac.uk/cru/data/nao/). The most recent updates are gathered on the website of Tim Osborn, Reader at CRU. We obtained the Jones et al. (1997) NAO winter index that considers the stations at Gibraltar and Reykjavik (http://www.cru.uea.ac.uk/timo/datapages/naoi.htm). The winter index from 2006/07 was distinctly positive, and the winter index from 2009/10 is one of the greatest negative values within the 190-year record (Table 1).

4 Methods

4.1 VTCI definition

VTCI was developed for monitoring the spatial patterns of agricultural droughts. It integrates remotely sensed information on surface reflectance (NDVI) and thermal land properties, taking advantage of both a change in LST and NDVI based on NDVI–LST space (Wan et al. 2004; Patel et al. 2011). Mathematically, the VTCI can be formulated as (Wang et al. 2001; Wan et al. 2004):

$$\text{VTCI} = \frac{\text{LSTNDVI}_{i \cdot \max} - \text{LSTNDVI}_i}{\text{LSTNDVI}_{i \cdot \max} - \text{LSTNDVI}_{i \cdot \min}} \qquad (1)$$

where

$$\text{LSTNDVI}_{i \cdot \max} = a + b * \text{LSTNDVI}_i \qquad (2)$$

$$\text{LSTNDVI}_{i \cdot \min} = a' + b' * \text{LSTNDVI}_i z \qquad (3)$$

LSTNDVI$_{i \cdot \max}$ and LSTNDVI$_{i \cdot \min}$ are the maximum and minimum LST of a certain NDVI LSTNDVI$_i$ to be found in the study area and represent the driest (upper edge) and wettest pixels (lower edge) in the NDVI–LST scatter plot, respectively. Physically, pixels with a low NDVI value correlate to bare soil and the surface on the upper end of the NDVI scale corresponds to densely vegetated areas with a transition area in-between (Fig. 2, upper left panel). Temperature variability impacts on evapotranspiration and soil moisture (Park et al. 2004) making, for instance, bare soil dry at a LST value close to the warm edge and wet at a LST close to the cold edge. Bare soil has a greater variability of LST values than densely vegetated areas, where plant cover extenuates the occurrence of high LST. In Fig. 2, we show the LST–NDVI scatter plot of four different land cover types from Jul 1 2004: Agricultural areas (non-irrigated agricultural lands and permanent crops) affiliate to less-vegetated areas and constitute the driest pixels together with the aggregated classes of natural grasslands and sparsely vegetated areas (Fig. 2, upper panels). Forests settle
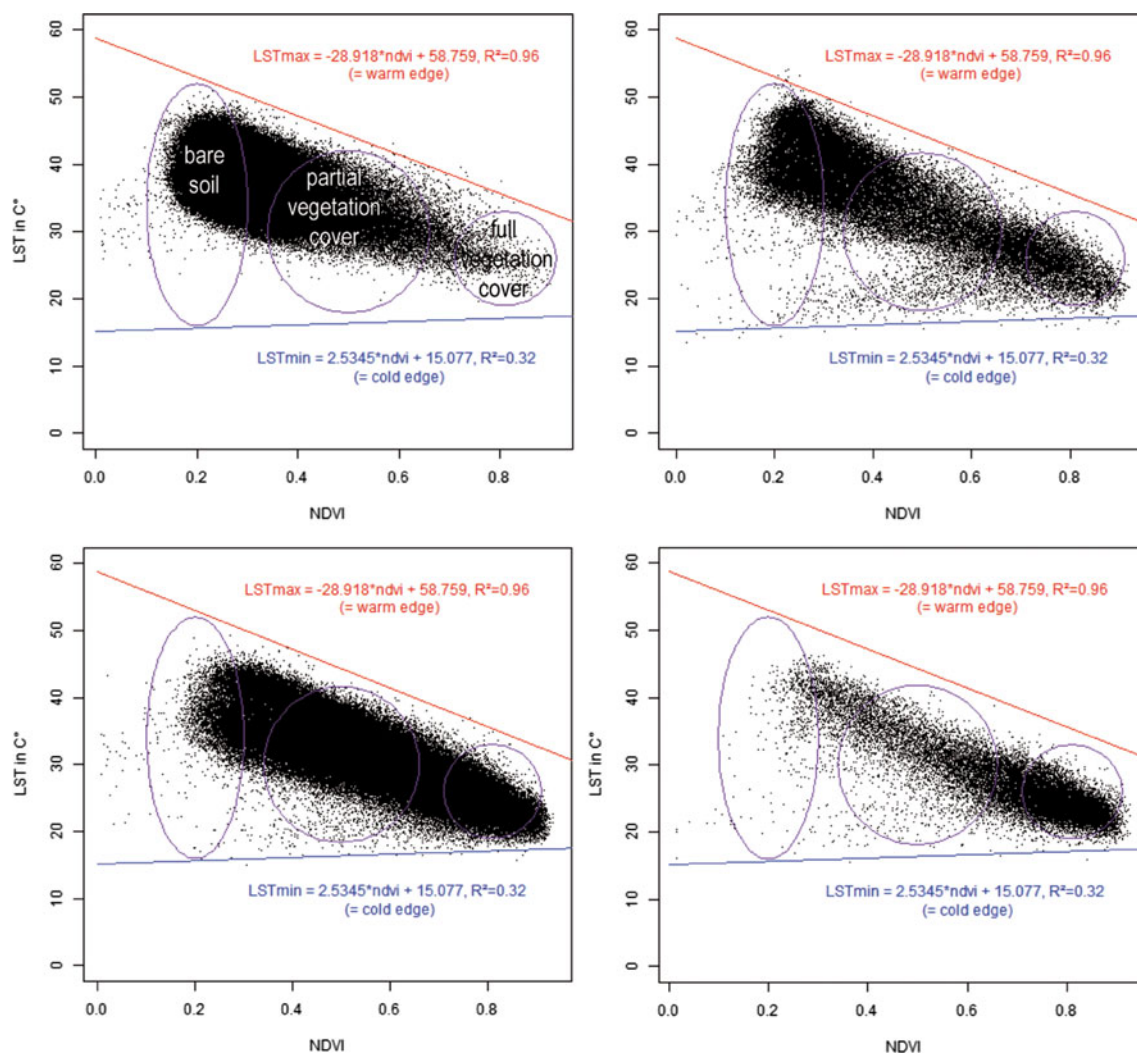
Fig. 2 NDVI–LST scatter plots from Jul 1 in 2004 for agricultural lands (non-irrigated agricultural areas and permanent corps), natural grasslands and sparsely vegetated areas, forests as well as pastures, moors and heathlands from the *upper left* to the *bottom right*. The plots include the

determined Eq. 1, Eq. 2 and R^2 of the complete NDVI and LST values from the observation date. The kind of vegetation cover as per theory (bare soil, partly and fully vegetated areas) is named only in the *upper left panel*

between a broad range from densely to fully vegetated areas, while pastures and moors that typically spread in northern Iberia represent one of the *moistest* land cover type (Fig. 2, lower panels).

4.2 Calculation of cold and warm edge

The determination of the cold (Eq. 2) and warm (Eq. 3) edge is crucial for calculating the VTCI. VTCI is a time-dependent and region-specific drought index that performs better during the plant growing season (Wan et al. 2004). We followed the strategy of Patel et al. (2011) and computed the coefficients for each observation date separately. For the computation, we produced a table indicating the LST–NDVI pair for each pixel. According to Patel et al. (2011), we sorted the columns by NDVI intervals (0.01) and extracted the maximum and minimum LST for each interval. Then, we improved their

approach by also extracting the *exact* NDVI value for each maximum and minimum LST. We chose the maximum and minimum LST with the corresponding (exact) NDVI value to calculate the cold and warm edge function via the Ordinary Least Squares (OLS) method. For obtaining a better coefficient of determination (R^2), we manually excluded extreme values and tails. Negative NDVI values were generally neglected. The coefficients a and a' are the intercepts, and the coefficients b and b' are the slope of the warm and cold edge, respectively. The average R^2 for all observation dates of the warm edge is 0.82, which implies that the variability of LST for dry pixels is well explained by NDVI. The slope of the cold edge approximates a horizontal line, whereby R^2 settles around 0. On the cold edge, the intercept offers more significant information than the slope. Figure 2 shows the linear regression lines for Jul 1 2004 including the equations (Eq. 2 and Eq. 3) and R^2.

The procedure described above was used to compute each of the 83 VTCI maps considered in this study. Every pixel in the maps presents a proper VTCI value.

4.3 VTCI interpretation

VTCI ranges between 0 and 1 with low values indicating severe vegetation stress and a value of 1 indicating no vegetation stress. In the literature, a VTCI threshold of 0.4 or 0.45 is used to indicate the start of vegetation stress due to drought (Wang et al. 2001; Sun et al. 2008; Patel et al. 2011). We considered pixels below a VTCI of 0.4 as dry pixels. Unlike previous studies, our study area accommodates a variety of habitats exhibiting soil moisture conditions from arid to wet; thus, we established equal drought categories utilising the entire VTCI spectrum. The four drought categories are very dry (VTCI 0–0.2), dry (VTCI 0.2–0.4), moderate (VTCI 0.4–0.6) and wet (VTCI 0.6–1). An equal interval classification was considered justified because the literature does not yet offer a definition of VTCI levels.

4.4 Correlation analysis

We computed the Pearson's correlation coefficient between NAO and VTCI pixel-wise using the different NAO winter indices of the observation years and the VTCI maps of one observation date during the entire study period. The point correlation analysis was repeated for all observation dates (Mar 1, Mar 2,…, Aug 2). In this manner, we produced 12 correlation maps of VTCI versus NAO for every observation date, where every pixel was assigned a Pearson's correlation coefficient r. According to Gouveia et al. (2008), pixels with a statistically significant (linear) correlation (significance levels of 10 % and less) will be named North Atlantic High Correlation pixels (NHCP).

4.5 Map production

All monthly or seasonal maps were obtained as an average from single observation maps. If pixels of one date were not available due to cloudy conditions, we omitted those pixels and considered only the values of the other VTCI map(s). If a pixel was empty in all source maps, it also remained blank in the average map.

5 Results and discussion

5.1 VTCI time series

The full collection of 83 VTCI maps is classified in ten equal intervals (0.1) ranging from 0 to 1 in order to preserve a grade of detail in the maps higher than four drought categories (see online Supplementary Data). The very dry class is kept in red colour tones, the dry class in orange colour tones, the moderate class in green colour tones and the wet class in blue colour tones. Because of space restrictions, in the paper, we only present monthly VTCI maps averaged by reference years (Fig. 3) but will consider the entire time series in the comments. Two thirds of the Iberian Peninsula respond to a typical Mediterranean climatic situation with spring months receiving irregular precipitation and summers becoming gradually dry during at least 2 months (Ceballos et al. 2004; Costa and Soares 2009; Costa et al. 2012). The north and northwest of the Iberian Peninsula are influenced by Atlantic Ocean Climate and also exhibit consistently higher VTCI during the warm season. March appears as the driest month in spring, particularly in western Iberia and along the east coast between Almeria and Alicante. In fact, a considerable negative trend of precipitation of up to 50 % in early spring is reported for the Iberian Peninsula and particularly its western parts in the second half of the twentieth century until the year 2000 triggered by a decline of cyclones moving from the Azores towards the Iberian Peninsula (Paredes et al. 2006; González-Hidalgo et al. 2010). A low VTCI in this sector is also reflected by the March maps during the last decade.

Land mass and relief play an important role in Iberian local VTCI manifestations. Major elevation systems also keep favourable soil moisture content during the warm season even in the traditionally dry parts in the south and east of the Iberian Peninsula, while sheltered areas within the main circulation direction consequently exhibit (very) dry conditions together with some wet phases in spring. The cloud blocking effect of mountains causes enhanced precipitation amounts and responds with a higher VTCI, whereas a rapid change from a high VTCI to a minor value may occur within a short distance. A sudden alternation from dry to moderate soil conditions is exemplified inland of the central Portuguese coast in March and April (Fig. 3), where the elevated areas of the Central System abruptly enter the coastal plain on a north–south orientated line and catch moisture content superior to the flat areas. The major basins (Figs. 1 and 3) constitute the most important lands for agricultural production in the Iberian Peninsula (Moratiel et al. 2011), but invariably extend in the lee of mountains or are located in climatically dry parts of the territory (Guadalquivir Basin, Tagus Basin). The Duero Basin in the northwest of the Iberian Peninsula represents the only plain exhibiting moderate conditions for vegetation in spring with some variability throughout the rest of the year. On the other hand, the blocking situation of the Pyrenees, Cantabrian Range and Iberian System turns the Ebro Basin in the northeast of Spain into Europe's most northern semi-arid region (Vicente-Serrano 2007) that demonstrates great instability between dry and wet phases in spring. In the time series, the beginning of May is often identified as the moistest period in the Ebro Basin and expresses the accumulated precipitation
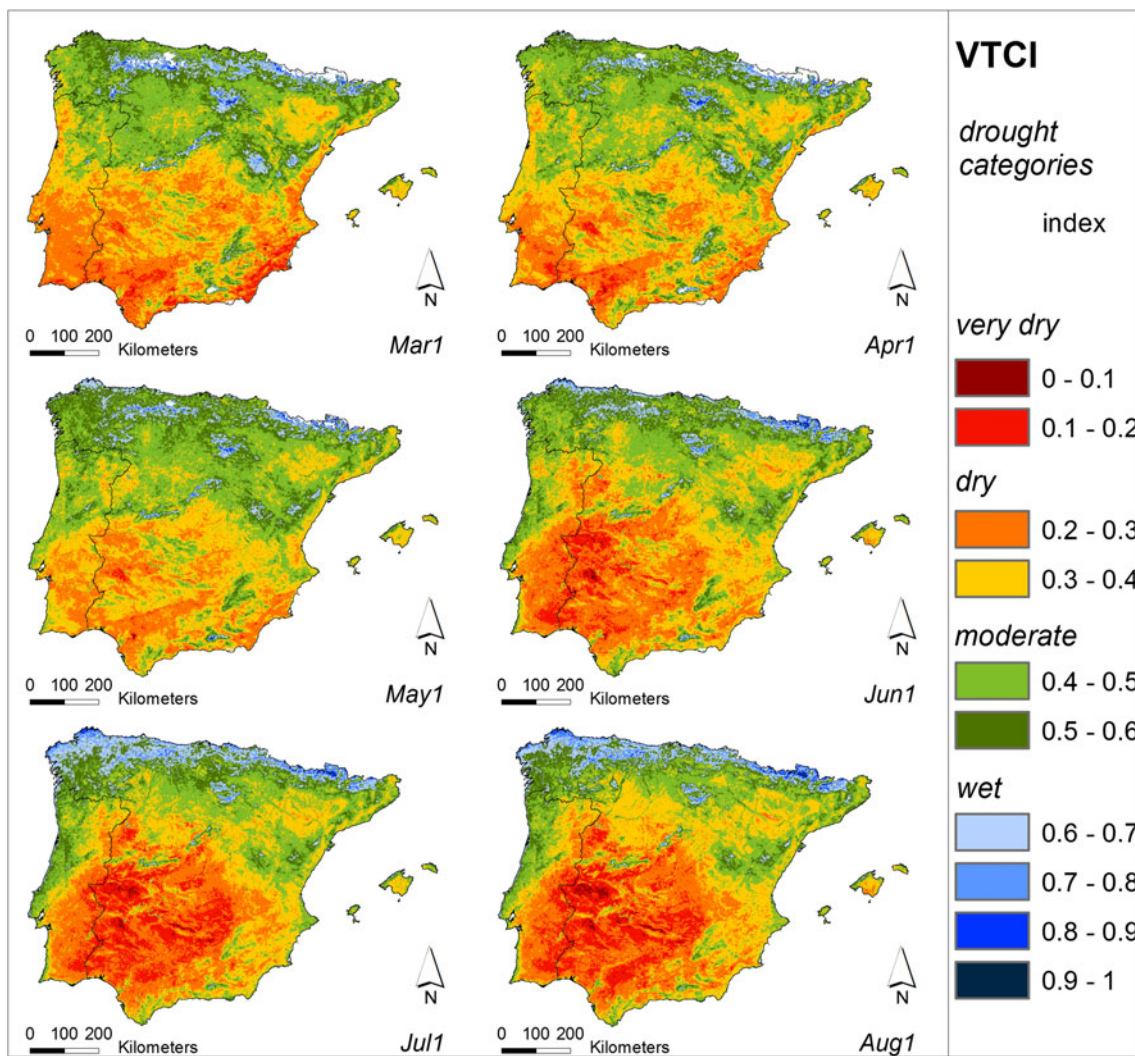
Fig. 3 Monthly average VTCI maps. The colour scheme refers to the established drought categories (very dry in *red colours*, dry in *orange colours*, moderate in *green colours* and wet in *blue colours*)

amounts from March to April that affect VTCI with a lagged time response in the last spring month (Vicente-Serrano 2007).

Figure 4 (upper panel) visualises the VTCI averaged by the entire territory in the course of the study period. The red horizontal line indicates the 0.4 threshold for discriminating dry and non-dry conditions. Major parts of the Iberian Peninsula are dry over extended parts of the year. Early spring mostly reveals less soil moisture than subsequent months, whereas 2001, 2005 and 2010 began particularly dry and were negative NAO (NAO−) years. VTCI exceeds the 0.4 threshold only during late spring months (April and May) but with a temporal irregularity characteristic for the Mediterranean climate (Ceballos et al. 2004; Paredes et al. 2006; Costa et al. 2012). The years 2003 and 2004 count as the wettest springs, while in 2007 and 2010, the dry period started very early already in mid-spring.

Drought categories show the distribution of dry and non-dry land at a higher grade of detail than average VTCI values. The course of drought categories over the study period on a monthly scale permits the detection of differences within the months (Fig. 4, lower panel). The Mediterranean climatic cycle is clearly identifiable by the increase of very dry areas during the summer months and a simultaneous reduction of moderate soil moisture conditions. Together with wet phases in early spring (2003, 2004) or late spring (2002, 2005, 2010), the dry category dominates surfaces of moderate soil moisture throughout the year and ranges between 45 and 60 %. The moderate category varies between 30 and 40 % with peaks of around 50 % in spring. In such dry years as 2001 and 2007, the gap between dry and moderate surfaces increases considerably, while the dry year 2005 was specifically marked by a low soil moisture level in March and the highest percentage (17.5 %) of very dry areas in August. The wet category is
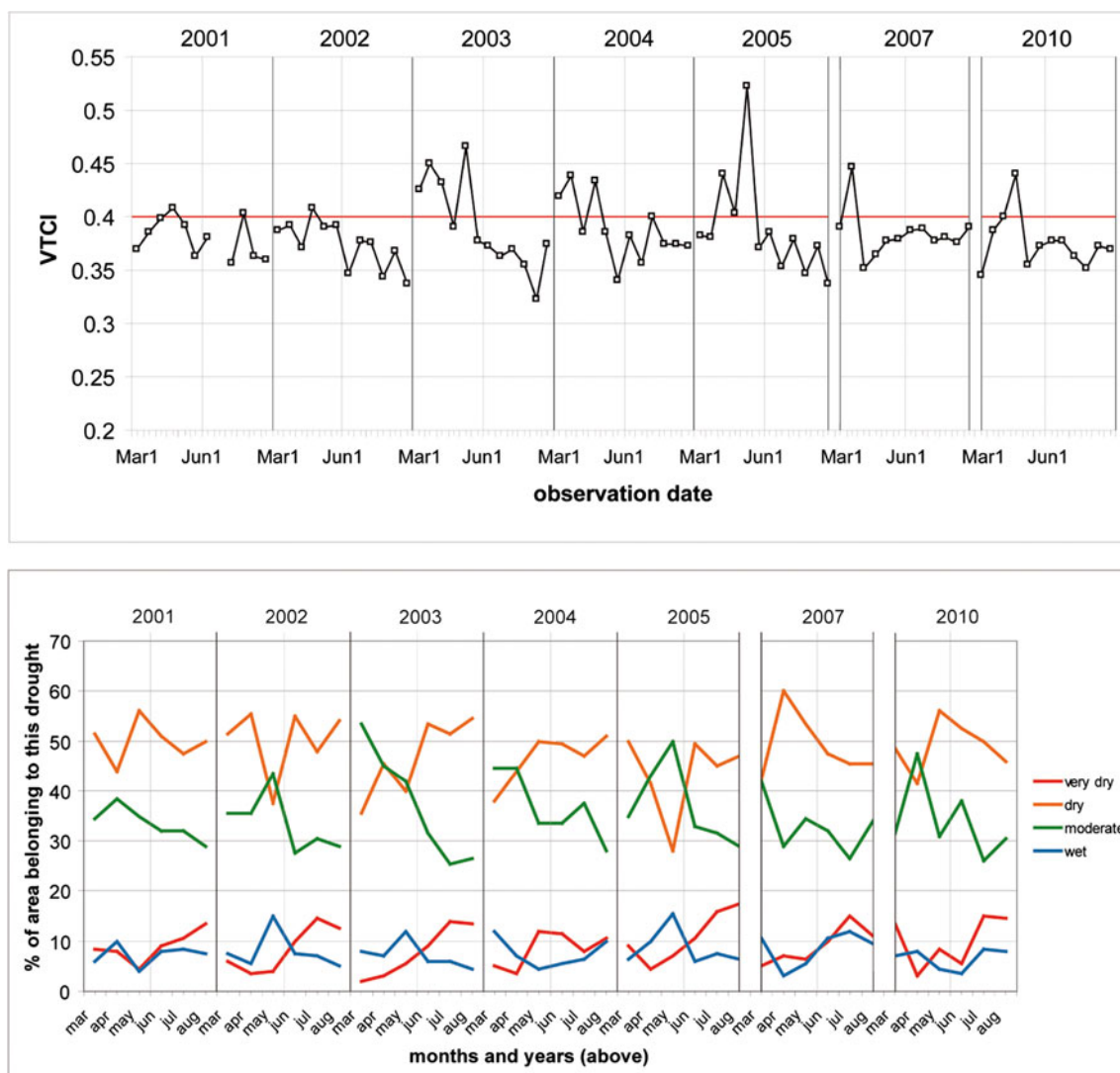
Fig. 4 Annual VTCI course during the reference period averaged by entire study area. The *red line* marks the 0.4 threshold for defining dry and non-dry areas (*upper panel*). Monthly surface cycle for drought categories (in %) during the reference years (*lower panel*)

normally greatest in mid-spring, thus reflecting humid spring situations. Wet conditions in summer are seen particularly in the north and northwest of the Iberian Peninsula where sufficient rainfall supports enhanced vegetation activity (Fig. 3).

Figure 5 portrays a small-scale VTCI detail of the Ebro Basin during a dry spring in Apr 1 2002 (upper panel). Very dry areas are scattered in the flat parts of the Ebro Basin (centre box), while surrounding mountains (Sierra Urbión and Parque Natural del Alto Tagus in Iberian System, Pyrenees) remain wet (left box). One month later, in May 1 2002 (Fig. 5, middle panel), the plain areas apparently profited from rainfall and exhibited moister conditions. In the agriculturally dominated flat landscape, forests and permanently irrigated agricultural lands are less sensitive to drought, as indicated by a higher VTCI in the small boxes at the dry date (Fig. 5a, b, upper panel) than in surrounding areas (Fig. 5, centre box). Mountain forests maintain favourable soil

moisture conditions in both dates (Fig. 5, left box). A characteristic situation is caused by relief along the east coast of the Iberian Peninsula where clouds from the main circulation direction release moisture in the blocking mountain ranges and leave the coastal areas much drier (Fig. 5, right box). The described situations from Fig. 5 are in line with Vicente-Serrano (2006), who found that apart from the main droughts that afflicted large areas in the Iberian Peninsula, the disaster tends to occur locally and typically permits the detection of a strong gradient between dry and wet soil conditions within short distance depending on preconditions such as land cover type and topography.

5.2 NAO versus VTCI

NAO has a known affect on climate in Europe and particularly on precipitation in the western Mediterranean Basin (Trigo
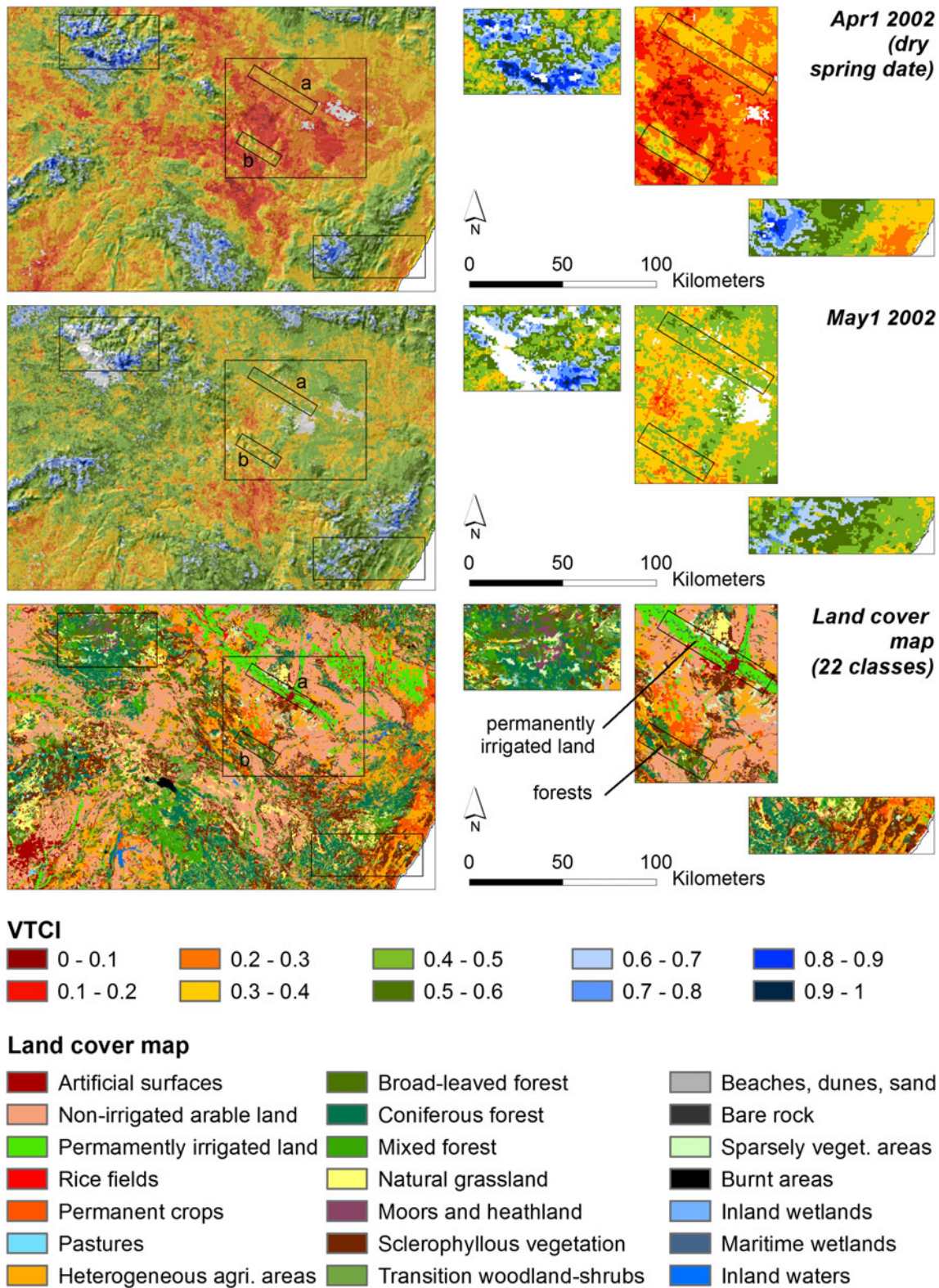
Fig. 5 VTCI maps of the Ebro Basin in the northeast of the Iberian Peninsula during a dry spring in Apr 1 2002 (*upper panel*) and 1 month later in May 1 2002 (*middle panel*); the land cover classes (CORINE land cover map 2006) are shown in the *lower panel*. The *box to the left* delineates mountainous areas of the Sierra de Demanda, Urbión, Cebollera and Cameros. The *middle box* specifies flat areas with irrigated agricultural areas (*upper small box*) and forests (*lower small box*). The *box on the right* marks relief along the east coast

et al. 2002; Paredes et al. 2006; Gouveia et al. 2008). The NAO winter index controls rainfall during the winter and spring months. Because the Iberian land mass is huge and comprises regions with different climatic and ecological preconditions, the influence of NAO on the occurrence of drought might vary spatially and temporally. Positive NAO (NAO+) years are associated with drier atmospheric conditions and negative NAO (NAO−) years imply intensified rainfall in the western Mediterranean (Trigo et al. 2002; Gouveia et al. 2008; Rodríguez-Puebla and Nieto 2010). In our correlation maps, a positive Pearson's coefficient entails wet soil conditions at the respective pixel in NAO+ years (as VTCI increases), while a positive coefficient in NAO− involves less soil moisture (as VTCI decreases). Inversely, negatively correlated pixels connote a dry situation in NAO+ and wet conditions in NAO− years. The results demonstrate notable alterations in correlation patterns in the course from spring to summer. Spring is marked by variable correlation patterns compared to a more stable situation during summer. In March, the correlation is positive in large parts of the Iberian Peninsula from central south to north exhibiting a strong correlation around the most southern tip (between Gibraltar and Cadiz) and on the Balearic Islands. A strongly negatively correlated area was identified in the south-eastern Iberian System and in central Catalonia at the beginning of March. Both April dates manifest similar and the most distinctive correlation patterns of all months featuring great differences compared to March: a large strongly negatively correlated area was detected in the centre-northwest of the Iberian Peninsula, while the southeast is positively correlated to NAO. Southern Portugal and the northern Ebro Basin exhibit a somewhat negative correlation at the beginning of April, while in the second half, the areas of negative correlation spread towards the south-eastern Iberian System. The correlation in the following month is weak and at the beginning of May almost not existent in Portugal and, again, becomes very clear at the end of June, when it is contrary to April: the northwest is positively correlated, while the southeast and east show a positive correlation towards NAO. We explain this alternation by the establishment of the stable, subtropical high pressure zone in this region at the beginning of summer. From mid July to mid August, the correlation pattern is similar to June, but at less magnitude; in late August, the area of positive correlation in west Iberia shifts towards the centre, while the Portuguese and Galician coastlines remain negatively correlated. On a monthly scale, the greatest amount of high correlation pixels (NHCP) affirms the distinct correlation pattern in April and June with 8 % (45,000 km^2) and 6 % (33,000 km^2) NHCP of all pixels, respectively. In March, 5 % (32,000 km^2) exhibit a strong correlation, while the NHCP amount of the remaining months drops to 1–2 % (Fig. 6).

5.3 Role of NAO on drought

The correlation findings relate to local VTCI in the time series. April, in fact, was relative dry in the centre-northwest (Duero Basin) during the NAO+ years (as VTCI decreased) and relatively humid in the NAO− years (as VTCI increased). The year 2010 with a distinct negative NAO winter index registered the driest March in the northwest but became significantly humid in April reflecting the alteration in correlation pattern. March is also very likely to become dry on the Balearic Islands during NAO− (observed 2001, 2010). The year 2007, a strong NAO+ year, registered the wettest situation in the southeast, which coincides with the high positive correlation in this region. June and July recorded specifically wet conditions in the centre-northwest and dry situations in the southeast and east during NAO+ (2002, 2003 and 2007), while 2010 (strong NAO− index) registered a dry situation in the centre-northwest at the end of June and July and a specifically wet August in the east and northeast.

We analysed the impact of NAO on drought (VTCI) for significant pixels by taking the annual VTCI cycle for the NHCP during NAO+ and NAO− years. Figure 7 illustrates the monthly average VTCI of NHCP for spring (upper panel) and summer season (bottom panel). The annual cycle of monthly mean VTCI for all reference years is indicated by the grey line, while the average cycle for the NAO+ (NAO−) subset is represented by the orange (blue) line. For both NHCP types (spring and summer), April implies the highest difference of VTCI between NAO+ and NAO−, whereas NAO+ Aprils turn out to be drier than NAO−. The findings coincide with observations from Gouveia et al. (2008), who discovered that NAO has the highest influence on NDVI in April enhancing (diminishing) vegetation activity in NAO− (NAO+) years. Indeed, the mean VTCI for all pixels of the Iberian Peninsula was lowest of all in April 2002 and 2007 (NAO+ years), while 2001, 2005 and 2010 (NAO− years) counted for humid Aprils. The month of April constitutes the period of the year that is characterised by intense vegetation activity and greatly impacts vegetation growth (Ji and Peters 2003). In contrast to spring, summer shows little fluctuation of NHCP during NAO+ and NAO−, which may be explained by the region-wide establishment of a stable high pressure zone during the summer months in contrast to the irregular occurrence of wet spells in spring.

The correlation of NAO versus a vegetation index (NDVI) produces different results compared to the correlation of NAO towards the drought index VTCI. Gouveia et al. (2008) found a persistent negative correlation between NAO and NDVI implying low (high) vegetation activity in spring and summer when NAO winter index was positive (negative). According to the authors, the NAO influence was the most notable in April, when in NAO+ years, vegetation activity was reduced compared to NAO− years. NAO versus VTCI correlation
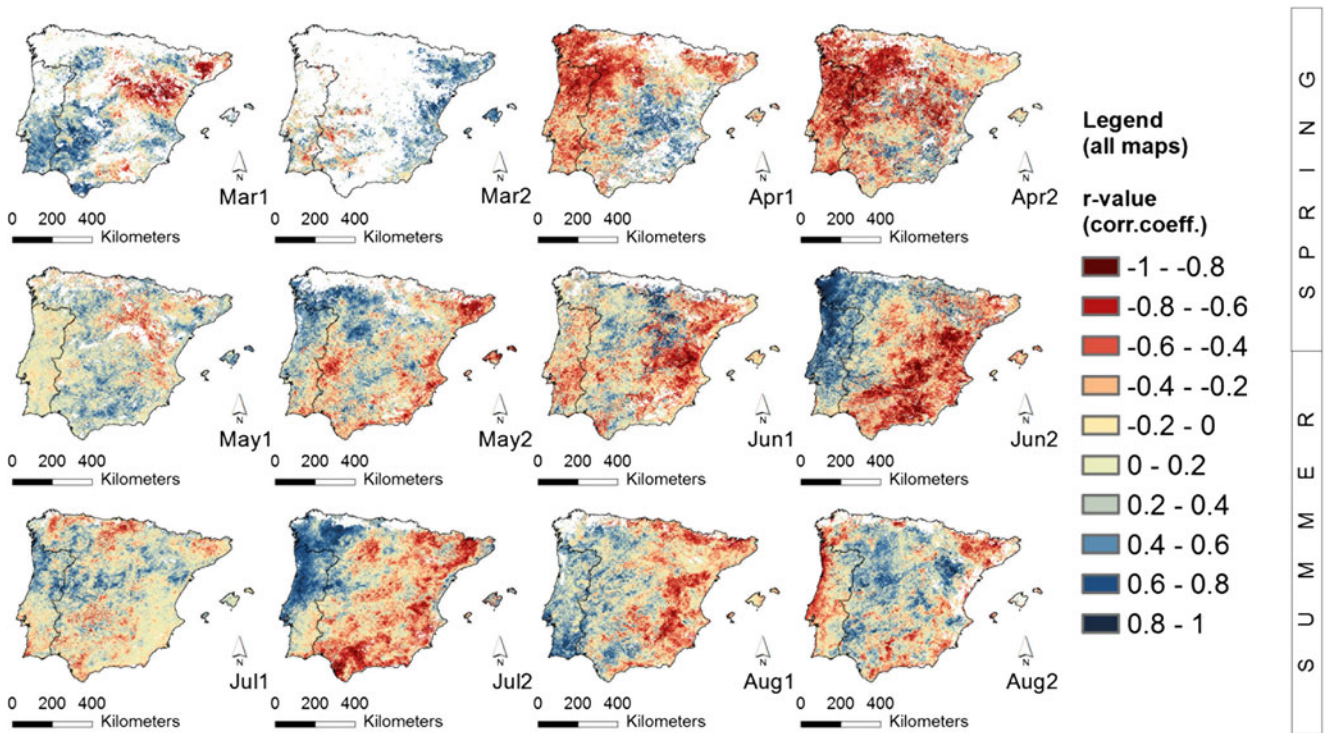
Fig. 6 Correlation maps of VTCI versus NAO per observation date

results in a clearly dipolar situation between April and June/July. In those 2 months, the northwest and southeast of the Iberian Peninsula exhibit an evidently opponent correlation one to each other, whereas the type of correlation reverses in the course of the seasons. Both indices, NDVI and VTCI, indentify April as drier (moister) during NAO+ (NAO−) years (Fig. 7). Vicente-Serrano and Heredia-Laclaustra (2004) describe a high correlation between NAO and the sum of NDVI
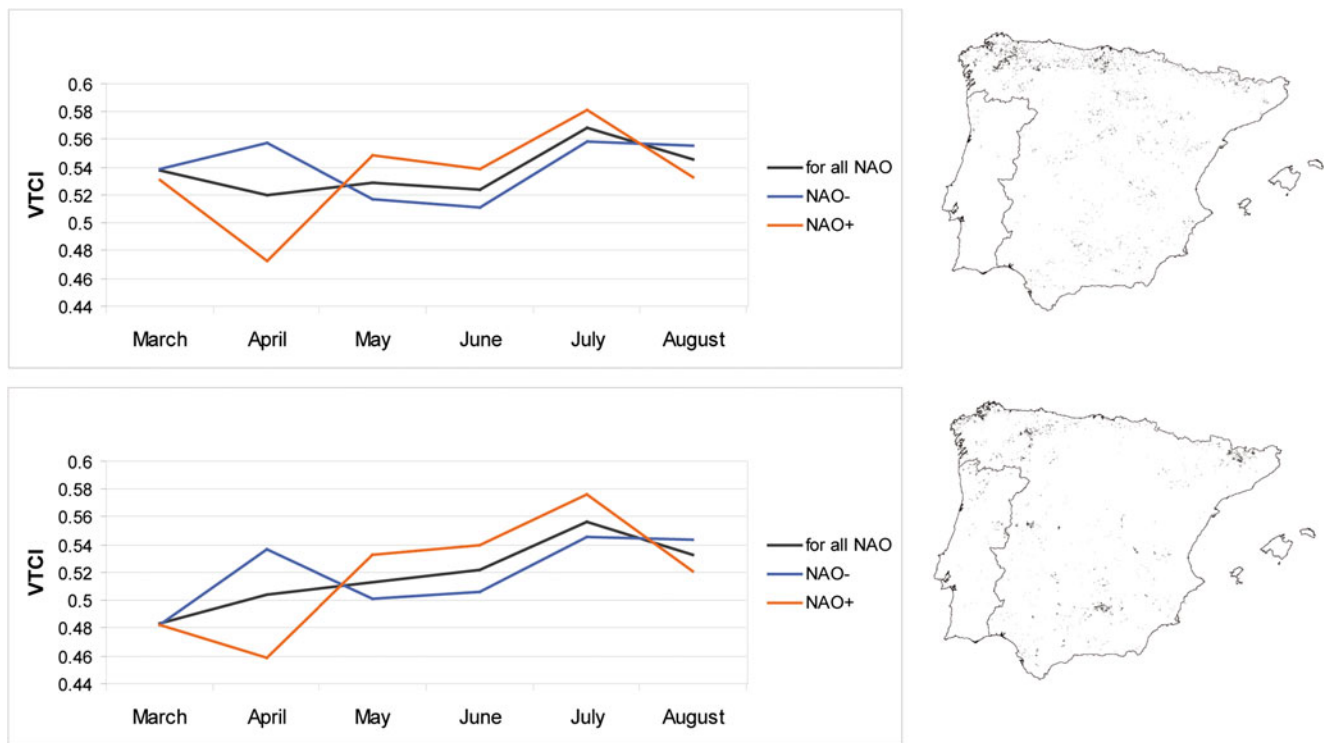

Fig. 7 Annual cycle of monthly VTCI for NHCP in spring (*upper panel*) and summer (*lower panel*). The maps aside localise the respective NHCP type (spring or summer)

for the study years 1982–2002 in the southwest and a non-significant correlation in the north. Contrarily, the southwest exhibits a less significant correlation between NAO and VTCI, whereas, as previously mentioned, the northwest is strongly correlated. Due to drought impact, the authors describe the southwest as an area with stable or slightly decreasing vegetation activity. The persistent occurrence of dry situations even during spring could be a reason for the weak correlation between VTCI and NAO in this region. In the previously mentioned studies, the authors investigated different study periods (1982–2002 and 1982–2000, respectively) based on NDVI, which could explain the different results. At this point, we also wish to stress that those studies examined the impact of climatic variables on large-scale vegetation dynamics, in order to predict vegetation trends. We applied the VTCI to identify local drought patterns and to estimate the impact of NAO on the occurrence of locally severe soil moisture conditions and therefore also used data of higher spatial resolution.

The high spatial and temporal variability of wet periods in spring prevents showing a clear correlation pattern especially in May and March. During these months, one area can be wet in one year but dry in the next. The prevailing Mediterranean climate with dry summers causes a clearer NAO influence pattern during the warm season, as the lack of precipitation during winter is decisive for a rapid increase in the accumulated precipitation deficit (Santos et al. 2007). The importance of April and other spring months is shown by the high impact on vegetation activity. The prominent role of water availability as a limiting factor for vegetation growth during spring is replaced by other determinants, such as low temperature and frosts in the remaining seasons. Droughts that occur in autumn and winter are therefore less influential than in spring and summer (Vicente-Serrano 2007). We believe that the extracted knowledge particularly for areas of high correlation between VTCI and NAO in spring could be useful for an early warning or forecasting system of drought in agricultural management.

5.4 Land cover

We analysed the distribution of pixels for 12 different land cover types pursuant to our four drought categories (not shown). Agricultural lands (non-irrigated agricultural land, permanent crops, heterogeneous agricultural areas and permanently irrigated agricultural land) account for the land cover types most vulnerable to drought, which is indicated by a dominating dry category (50–80 %), a weak moderate category (10–45 %) and a negligible wet category throughout the year as well as a gaining very dry category in summer (up to 18 % for permanent crops and 16 % for non-irrigated agricultural lands). A missing vegetation layer makes those agricultural lands specifically sensitive to drought during growing period in early spring when the root system is still poorly

developed and soil easily runs dry. Unfavourable conditions in spring restrain cereals and root crops from healthy plant development and thus are liable to diminished harvests (Xoconostle-Cazares et al. 2010).

Of all land uses, forests constitute the land cover most resilient to drought. In the inter-annual profile of all forest types, the moderate class consistently has greater share than the dry one. Mixed forests appear most robust, but mainly extend in the humid areas of the Iberian Peninsula. Coniferous forests, on the other hand, exhibit favourable condition even in drier zones. Other than the native oak species, pine trees are able to cope well with the environmental conditions of a Mediterranean climate. Only broad-leaved forests become partly dry during summer.

For low vegetation types such as natural grasslands, sclerophyllous vegetation and sparsely vegetated areas (around 15 % of the Iberian Peninsula's surface), we detected a great fluctuation of soil moisture conditions within two subsequent observation dates in the VTCI time series, especially in spring (Fig. S1–S14). Low vegetation types react more sensitively to drought than high vegetation and are often located in areas with the highest aridity (Vicente-Serrano et al. 2006). These ecotypes compound species that developed strategies to outlast regular dry periods and are able to quickly expand when water is available because they promptly respond to spatiotemporal changes in soil moisture (Le Houerou 1996; Bonifacio et al. 1993; Sannier and Taylor 1998; Vicente-Serrano 2007), which explains the fluctuation in the VTCI maps. Because it is a near real-time drought index, VTCI proves advantageous for the spatiotemporal monitoring of permanently altering drought conditions.

The presented results are in line with findings of other authors, who argued that the effects of drought on vegetation are diverse and depend on the land cover type, the vegetation characteristics (mean NDVI), the month, the timeframe of the episode and the climatic conditions (Vicente-Serrano 2007; Gouveia et al. 2009). The frequent occurrence of drought enhances fire frequencies, soil erosion, degrades vegetation and is harmful for agriculture and economy (Wilhite et al. 2007; Costa and Soares 2012). Iberia's land cover types are to a great extent human induced. Wide areas of the landscape are dominated by agricultural lands and forms of low vegetation that often evolved as a degradation of forests. It is not unexpected that agricultural areas (specifically non-irrigated agricultural lands) constitute the land classes most afflicted by droughts. They were artificially created in areas separate from the environmental conditions that would support the growth of the respective vegetation and do not endure periods of drought. Bennie and Hensley (2001) reported that farms in regions with an average annual rainfall of less than 600 mm need to have a larger surface area than those in humid regions to achieve an equal output of crop harvest. In terms of economical value, agricultural lands constitute meaningful land cover types.

Thus, rising temperatures, decreasing amounts of rainfall and the intensification of agriculture in many parts of Spain during the second half of the last century will force the promotion of efficiency in irrigation methods and a change in crop models (Ceballos et al. 2004; Martín-Rosales et al. 2007; Lasanta and Vicente-Serrano 2012). Calculating the impacts of drought on agriculture is therefore crucial for determining consequences in water management, particularly in the context of climate change.

The usefulness of VTCI for assessing local drought conditions on agricultural land is shown in this section. Accommodating the largest adjacent area of non-irrigated agricultural land, the Duero Basin (region of Castilla and Leon) represents the most important region of agricultural production in Spain (Moratiel et al. 2011). With a cultivated area of 20,000 km², wheat (*Triticum aestivum L.*) and barley (*Hordeum vulgare L.*) comprise 70 % of the crop lands in the Duero Basin, whereas 90 % are non-irrigated. The Duero Basin embodies the typical 'Submeseta Norte', a territory of elevated average altitude (above an altitude of 700 m) with two distinct parts: a dry plain prairie region with around 400 mm annual average rainfall in the centre and humid surrounding mountainous areas (more than 1000 mm annual average rainfall). In Fig. 8, we highlighted soil moisture differences for non-irrigated agricultural lands between a normal year (2004) and a dry 2005. The normal year started favourably in March with great areas exhibiting a VTCI between 0.5 and 0.6, and more. The summer months become dry in the southern provinces, whereas the north-eastern parts retain favourable conditions. In contrast, 2005 began already very dry in the major central parts of the Duero Basin. In April, the situation modified opportunely and again became gradually drier after May. The summer and especially August of 2005 were to a great extent dry. Wide areas across Spain suffered from accumulated hydrological drought in the early spring of 2005 and 2006 (Ceballos-Barbancho et al. 2008). This observation became more frequent for the southwest sector of the Duero Basin in recent decades. The authors reported a decrease in rainfall between November and March (statistically significant in February and March) since the late 1950s. Indeed, the harvest of cereals in Castilla and Leon was 3600 kg/ha in 2004 and only 2280 kg/ha in 2005 (EUROSTAT 2013).

Droughts in spring are more influential than in other periods of the year because the cumulative precipitation deficiency hinders a quick start into the growing season (Vicente-Serrano 2007). In 2005, the humid April apparently could not compensate the lack of rainfall in late winter/early spring. Figure 9 below points to the anomalies of VTCI in 2005 with respect to the average time
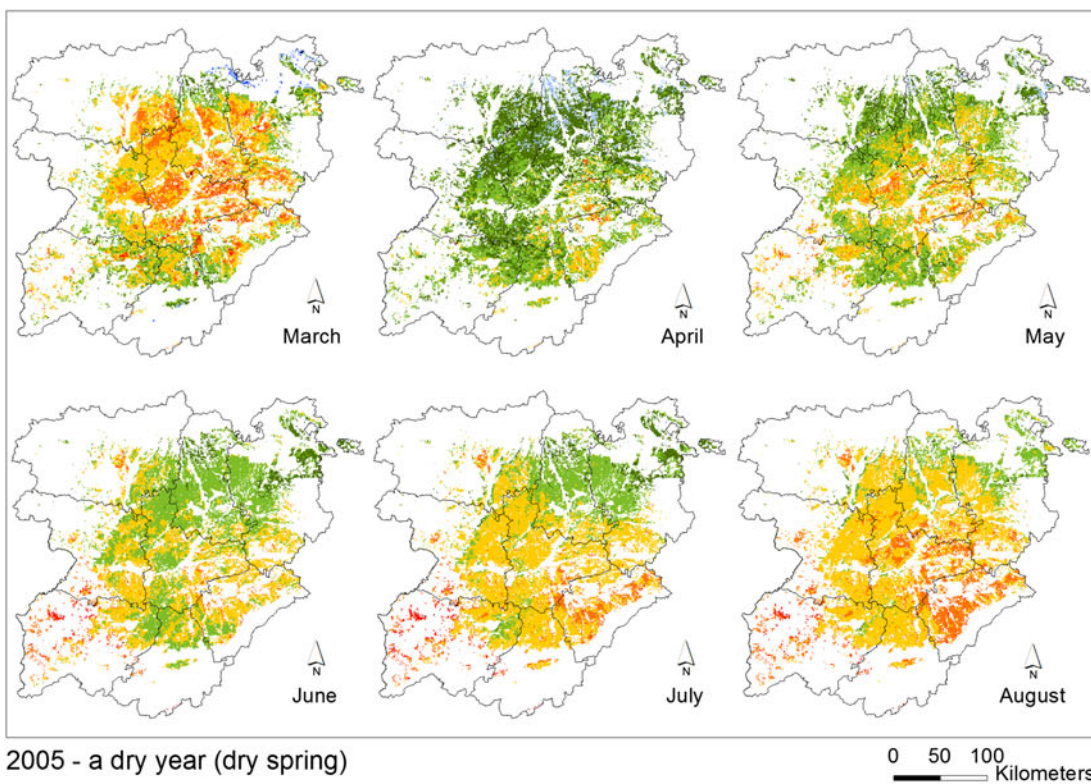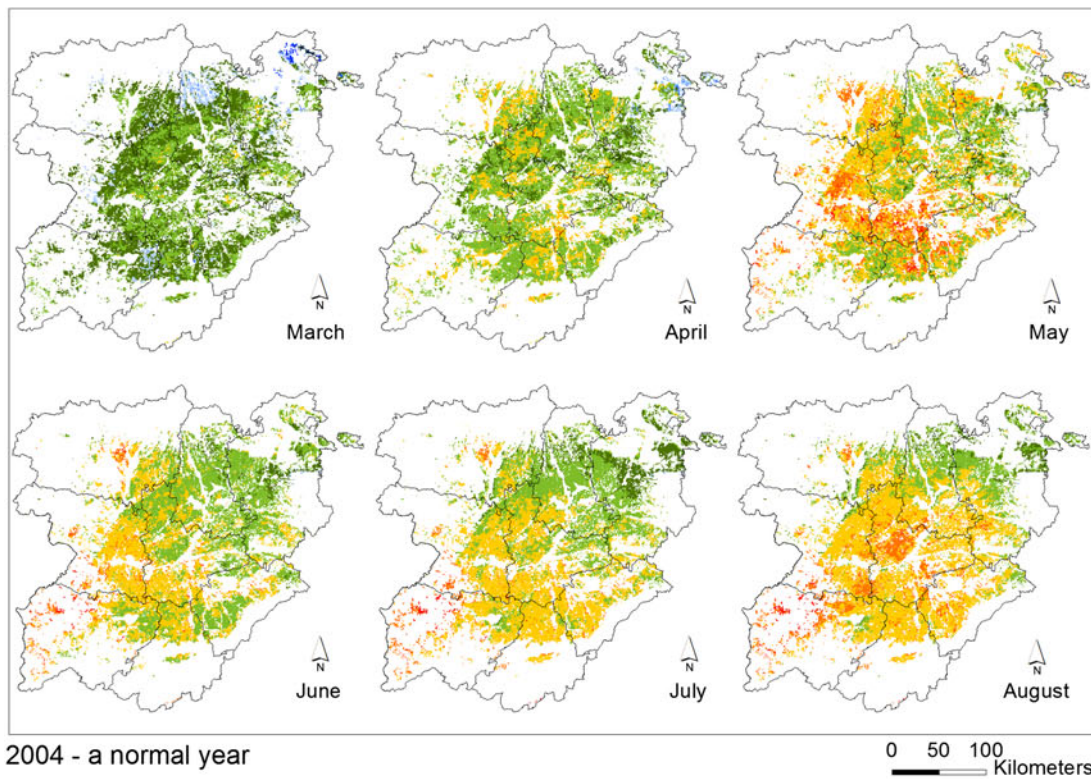
Fig. 8 Monthly VTCI of non-irrigated agricultural lands in the Duero ▶ Basin (northwest of the Iberian Peninsula) during a normal year (2004, *upper panel*) and a dry year (2005, *lower panel*)

series of non-irrigated arable surfaces all over the Iberian Peninsula. A positive (negative) difference of VTCI connotes drier (more humid) conditions in 2005 and is marked as red (blue). The cited VTCI indicates the magnitude of the anomaly. According to Fig. 9, major parts of the Duero Basin were drier during 5 of 6 months in 2005 compared to an average year and specifically dry in March (a VTCI of less than 0.2). Only April appeared wetter than an average month, which coincides with the negative correlation to NAO− in this region (as VTCI increases; Fig. 8). A VTCI land cover study is also efficient in highlighting the spatial differences of droughts: while the Duero Basin was drier in 2005, the Ebro Basin simultaneously exhibited wetter conditions compared to an average year.
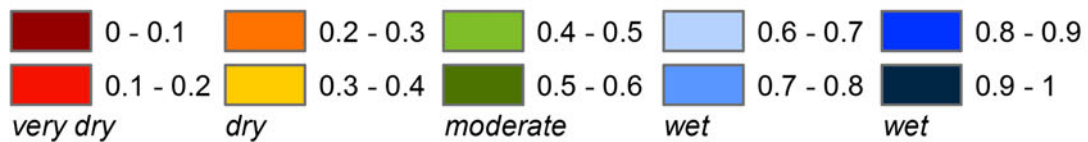
5.5 NAO and land cover

We showed the high influence of NAO on VTCI in April. At the same time, the importance of April is given by the high impact on vegetation activity specifically on non-irrigated agricultural lands. In Fig. 10, we exemplify the high correlation areas of NAO versus VTCI in the centre-northwest for April of all years, which coincide with the vast areas of non-irrigated agricultural lands in the Duero Basin. The box in Fig. 10 marks the negatively correlated area, whereas the solid (dashed) line represents NAO− (NAO+). To recapitulate, a negative correlation coefficient implies dry (moist) conditions during NAO+ (NAO−) as VTCI decreases (increases). Indeed, the VTCI maps from Apr 1 and Apr 2 in 2002 and 2007 (both NAO+) show dry areas in the northwest, while the same region was considerably moister during NAO− (2001, 2005, 2010). The years 2003 and 2004 were indistinct with specifically Apr 2 2003 and Apr 1 2004 falling beyond the correlation pattern. However, the Duero Basin is very likely to experience dry conditions in a NAO+ April and favourable conditions during a NAO− April.

On a local scale, as represented by the Iberian Peninsula, the NAO–VTCI correlation pattern contributes important knowledge about the spatiotemporal variability of soil moisture conditions, especially in spring. Considering that NAO, as the major atmospheric circulation mode, controls rainfall events in the Western Mediterranean, this knowledge can be used to develop local drought warning tools for water management and agriculture based on a certain NAO winter index. At this point, we want to stress that such atmospheric circulation patterns as the NAO is not the only factor that acts on drought. The nature and quality of soil

2004 - a normal year   0   50   100 Kilometers

2005 - a dry year (dry spring)   0   50   100 Kilometers

VTCI

0 - 0.1	0.2 - 0.3	0.4 - 0.5	0.6 - 0.7	0.8 - 0.9
0.1 - 0.2	0.3 - 0.4	0.5 - 0.6	0.7 - 0.8	0.9 - 1
very dry	*dry*	*moderate*	*wet*	*wet*

VTCI difference between average years and 2005 for non-irrigated arable land

- -1 - -0.4
- -0.4 - -0.3
- -0.3 - -0.2
- -0.2 - -0.1
- -0.1 - 0
- 0 - 0.1
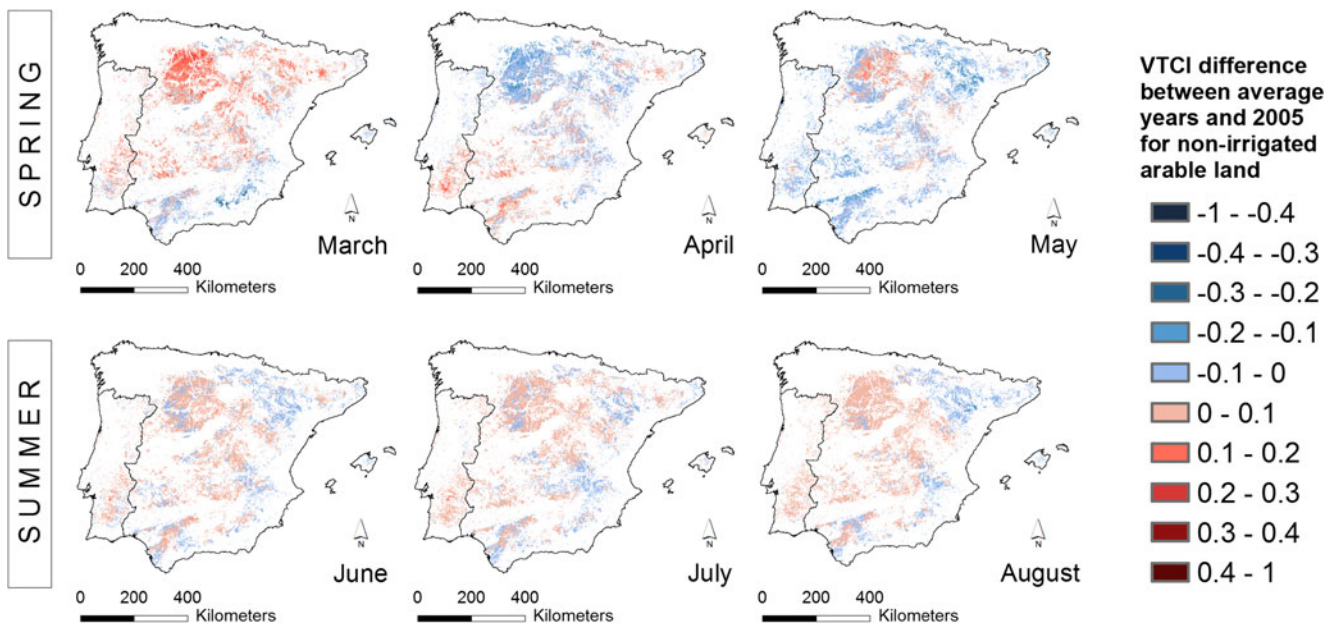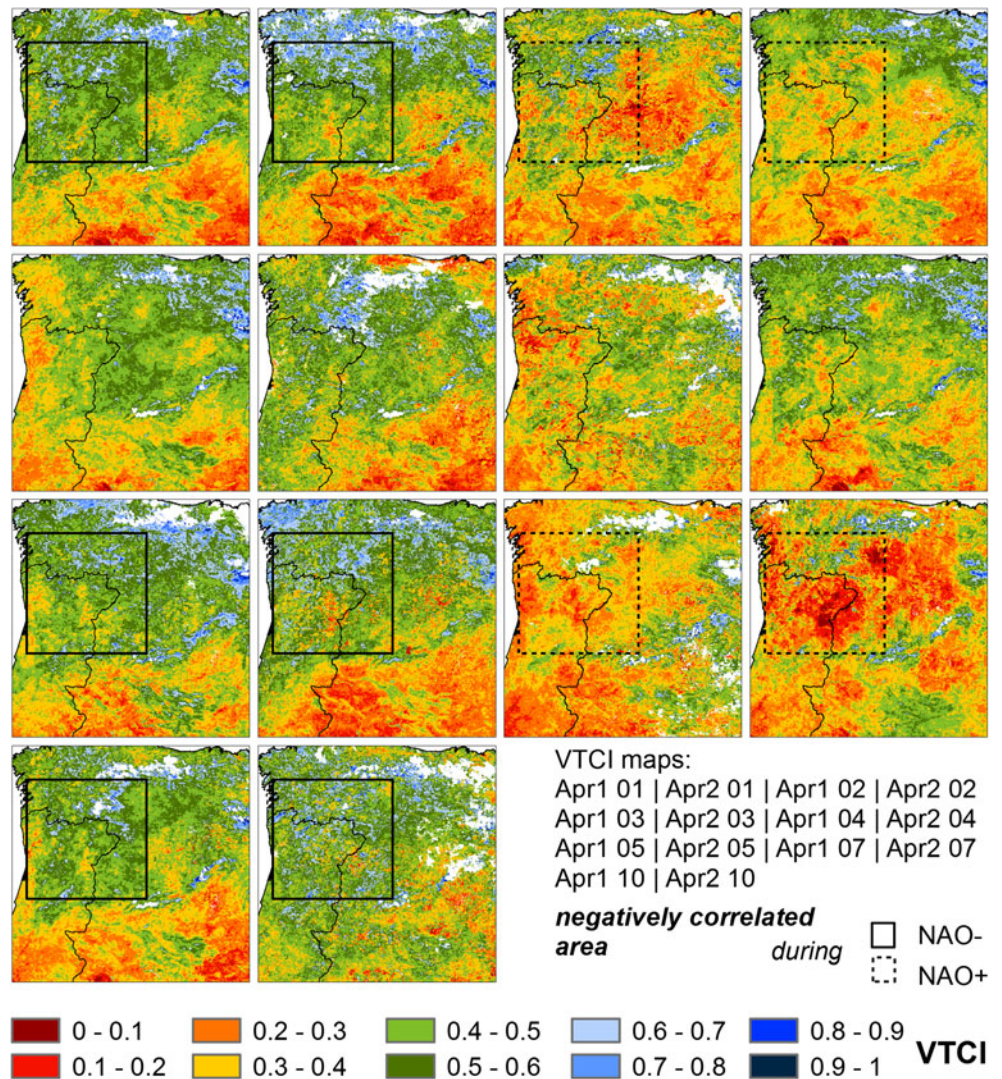- 0.1 - 0.2
- 0.2 - 0.3
- 0.3 - 0.4
- 0.4 - 1

Fig. 9 Anomalies of VTCI between an average year and a dry year (2005) for non-irrigated arable land

Fig. 10 Centre-northwest of the Iberian Peninsula with highly negatively correlated areas (*box*) during April dates for the years 2001–2005, 2007 and 2010. The *solid box* refers to NAO−, and the *dashed box* to NAO+

VTCI maps:
Apr1 01 | Apr2 01 | Apr1 02 | Apr2 02
Apr1 03 | Apr2 03 | Apr1 04 | Apr2 04
Apr1 05 | Apr2 05 | Apr1 07 | Apr2 07
Apr1 10 | Apr2 10

negatively correlated area   *during*   ☐ NAO−
                                            ⌐ ⌐ NAO+

VTCI
- 0 - 0.1
- 0.1 - 0.2
- 0.2 - 0.3
- 0.3 - 0.4
- 0.4 - 0.5
- 0.5 - 0.6
- 0.6 - 0.7
- 0.7 - 0.8
- 0.8 - 0.9
- 0.9 - 1

substrate, the intensive use of agricultural land and application of irrigation are human-induced influences that have an impact on the availability of water for plants (Gouveia et al. 2008).

6 Conclusions

This study investigates the occurrence of spatiotemporal drought patterns in the Iberian Peninsula within the last decade using Vegetation Temperature Condition Index (VTCI). The role of North Atlantic Oscillation on local drought occurrences was subject to further study. Despite its link to vegetation activity (NDVI), the VTCI was specifically developed to locate areas that provoke vegetation stress associated with drought. The VTCI results reflect a Mediterranean annual cycle in major parts of the terrain and an Atlantic-influenced section in the north and northwest. Relief highly impacts the establishment of dry areas, whereas the conditions may vary within a short distance. We also made evident that the application of VTCI enables the spatiotemporal detection of drought as a highly variable phenomenon and facilitates the identification of soil moisture conditions at a small (local) scale.

VTCI constitutes a less-probed drought index. For a region-wide use not limited to agricultural areas, an additional analysis of the calculation process, namely the establishment of the cold and warm edge that highly influence the index, would sustain its robustness.

Understanding the NAO influence on drought occurrences is particularly interesting for the spring season when vegetation activity is high and dependent on sufficient rainfall. The clear correlation patterns in March, April and June coincide with observations in the VTCI time series and are useful for understanding the spatiotemporal variability of droughts in relation to the large-scale NAO mode. We gave the example of the Duero Basin, where April is very likely to be dry (wet) in NAO+ (NAO−) as VTCI decreases (increases). The correlation findings may trigger the development of an advance warning system for soil moisture conditions, especially for spring months, which would be of great interest for drought management in agriculture. Therefore, further analysis should be applied to improve the knowledge of the relationship between NAO and VTCI. Although the computation of the VTCI is time consuming, the coverage of several decades could deliver important spatiotemporal information on soil moisture conditions for local analysis. We also suggest testing a NAO winter index that only considers December, January and February as an index by the beginning of March is already of interest for agricultural endeavour.

References

AEMET (2012) Website of the Spanish Meteorological Agency. www.aemet.es. Accessed February 2013

Bayarjargal Y, Karnieli A, Bayasgalan M, Khudulmur S, Gandush C, Tucker CJ (2006) A comparative study of NOAA-AVHRR derived drought indices using change vector analysis. Remote Sens Environ 105:9–22

Bennie ATP, Hensley M (2001) Maximizing precipitation utilization in dry-land agriculture in South Africa—a review. J Hydrol 241:124–139

Bonifacio R, Dugdale G, Milford JR (1993) Sahelian rangeland production in relation to rainfall estimates from Meteosat. Int J Remote Sens 14:2695–2711

Caccamo G, Chisholm LA, Bradstock RA, Puotinen ML (2011) Assessing the sensitivity of MODIS to monitor drought in high biomass ecosystems. Remote Sens Environ 115:2626–2639

Carlson TN, Ripley DA (1997) On the relation between NDVI, fractional vegetation cover and leaf area index. Remote Sens Environ 62:241–252

Carlson TN, Perry EM, Schmugge TJ (1990) Remote estimation of soil moisture availability and fractional vegetation cover for agricultural fields. Agric For Meteorol 52:45–69

Ceballos A, Martínez-Fernández J, Luengo-Ugidos MA (2004) Analysis of rainfall trend and dry periods on a pluviometric gradient representative of Mediterranean climate in Duero Basin, Spain. J Arid Environ 58:215–233

Ceballos-Barbancho A, Morán-Tejeda E, Luengo-Ugidos MA, Llorente-Pinto JM (2008) Water resources and environmental change in a Mediterranean environment: the south-west sector of the Duero river basin (Spain). J Hydrol 351:126–138

Choi M, Jacobs JM, Anderson MC, Bosch DD (2013) Evaluation of drought indices via remotely sensed data with hydrological variables. J Hydrol 476:265–273

Choudhury BJ, Ahmed NU, Idso SB, Reginato RJ, Daughtry CTS (1994) Relations between evaporation coefficients and vegetation indices studied by model simulations. Remote Sens Environ 50:1–17

Costa AC, Soares A (2009) Trends in extreme precipitation indices derived from a daily rainfall database for the South of Portugal. Int J Climatol 9(13):1956–1975

Costa AC, Soares A (2012) Local spatiotemporal dynamics of a simple aridity index in a region susceptible to desertification. J Arid Environ 87:8–18

Costa AC, Santos JA, Pinto JG (2012) Climate change scenarios for precipitation extremes in Portugal. Theor Appl Climatol 108:217–234

Dall'Olmo G, Karnieli A (2002) Monitoring phonological cycles of desert ecosystems using NDVI and LST data derived from NOAA-AVHRR imagery. Int J Remote Sens 23:4055–4071

Davenport ML, Nicholson SE (1993) On the relation between rainfall and the Normalized Difference Vegetation Index for diverse vegetation types in East Africa. Int J Remote Sens 14:2369–2389

EEA (2013) European Environmental Agency—CORINE Land Cover map 2006. http://www.eea.europa.eu/data-and-maps/data/corine-land-cover-2006-clc2006-100-m-version-12-2009. Accessed March 2013

EUROSTAT (2013) Website of Eurostat, a Directorate-General of the European Commission about European Statistics. http://epp.eurostat.ec.europa.eu/portal/page/portal/eurostat/home/. Accessed March 2013

Gao BC (1996) NDWI—a normalized difference water index for remote sensing of vegetation liquid water from space. Remote Sens Environ 58:257–266

Ghulam A, Qin Q, Zhan Z (2007) Designing of the perpendicular drought index. Environ Geol 52:1045–1052. doi:10.1007/s00254-006-0544-2

Gillies RR, Carlson TN, Cui J, Kustas WP, Humes KS (1997) A verification of the 'triangle' method for obtaining surface soil water content and energy fluxes from remote measurement of the Normalized Difference Vegetation Index (NDVI) and surface radiant temperature. Int J Remote Sens 18:3145–3166

Gonzalez-Alonso F, Calle A, Casanova JL, Vazquez A, Cuevas JM (2000) Operational monitoring of drought in Spain using NOAA–AVHRR satellite images. Proceedings of 28th International Symposium on Remote Sensing of Environment 27–31 March, Cape Town, South Africa

González-Hidalgo JC, Brunetti M, De Luis M (2010) Precipitation trends in Spanish hydrological divisions, 1946–2005. Clim Res 43:215–228

Goodess CM, Jones PD (2002) Links between circulation and changes in the characteristics of Iberian rainfall. Int J Climatol 22:1593–1615

Gouveia C, Trigo RM (2011) The Impacts of the NAO on the Vegetation Activity in Iberia. In: Vicente-Serrano SM, Trigo RM (eds) Hydrological, socioeconomic and ecological impacts of the North Atlantic Oscillation in the Mediterranean Basin. Springer Verlag, Berlin-Heidelberg-New York, pp 113–128. doi:10.1007/978-94-007-1372-7

Gouveia C, Trigo RM, DaCamara CC, Libonati R, Pereira JMC (2008) The North Atlantic Oscillation and European vegetation dynamics. Int J Climatol 14:1835–1847. doi:10.1002/joc.1682

Gouveia C, Trigo RM, DaCamara CC (2009) Drought and vegetation stress monitoring in Portugal using satellite data. Nat Hazards Earth Syst Sci 9:185–195. doi:10.5194/nhess-9-185-2009

Goward SN, Xue Y, Czajkowski KP (2002) Evaluating land surface moisture conditions from the remotely sensed temperature/vegetation index measurements: an exploration with the simplified simple biosphere model. Remote Sens Environ 79:225–242

Hurrell JW (1995) Decadal trends in the North Atlantic Oscillation and relationships to regional temperature and precipitation. Science 269:676–679

Jang JD, Viau AA, Anctil F (2006) Thermal-water stress index from satellite images. Int J Remote Sens 27:1619–1639

Ji L, Peters AJ (2003) Assessing vegetation response to drought in the northern Great Plains using vegetation and drought indices. Remote Sens Environ 87:85–98

Jones PD, Jonsson T, Wheeler D (1997) Extension to the North Atlantic Oscillation using early instrumental pressure observations from Gibraltar and South-West Iceland. Int J Climatol 17:1433–1450

Julien Y, Sobrino JA, Verhoef W (2006) Changes in land surface temperature and NDVI values over Europe between 1982 and 1999. Remote Sens Environ 103:43–55

Karnieli A, Dall'Olmo G (2003) Remote sensing monitoring of desertification, phenology and droughts. Manag Environ Qual 14:22–38

Karnieli A, Agam N, Pinker RT, Anderson M, Imhoff ML, Gutman GG, Panov N, Goldberg A (2010) Use of NDVI and land surface temperature for drought assessment: merits and limitations. J Clim 23:618–633

Kogan FN (1990) Remote sensing of weather impacts on vegetation in non-homogeneous areas. Int J Remote Sens 11:1405–1419

Kogan FN (1995) Application of vegetation index and brightness temperature for drought detection. Adv Space Res 15:91–100

Kogan FN (1997) Global drought watch from space. Bull Am Meteorol Soc 78:621–636

Kogan FN (2000) Contribution of remote sensing to drought early warning. In: Wilhite DA, Sivakumar MVK, Wood DA (eds) Early warning systems for drought preparedness and drought management. Proc. Expert Group Meeting, 5–7 September, Lisbon (Portugal). World Meteorological Organization, Geneve, pp 86–100

Lasanta T, Vicente-Serrano SM (2012) Complex land cover change processes in semiarid Mediterranean regions: an approach using Landsat images in northeast Spain. Remote Sens Environ 124:1–14

Lazzarini M, Marpu PR, Ghedira H (2013) Temperature-land cover interactions: the inversion of urban heat island phenomenon in desert city areas. Remote Sens Environ 130:136–152

Le Houerou HN (1996) Climate change, drought and desertification. J Arid Environ 34:133–185

Liu WT, Negron-Juarez RI (2001) ENSO drought onset prediction in northeast Brazil using NDVI. Int J Remote Sens 22:3483–3501

Lobo A, Ibanez Marti JJ, Carrera Giménez-Cassina C (1997) Regional scale hierarchical classification of temporal series of AVHRR vegetation index. Int J Remote Sens 18(15):3167–3193

Martín-Rosales W, Pulido-Bosch A, Vallejos A, Gisbert J, Andreu JM, Sánchez-Martos F (2007) Hydrological implications of desertification in southeastern Spain. Hydrol Sci J 52(6):1146–1161

Martins DS, Raziei T, Paulo AA, Pereira LS (2012) Spatial and temporal variability of precipitation and drought in Portugal. Nat Hazards Earth Syst Sci 12:1493–1501

Martín-Vide J, Fernández D (2001) El ídice NAO y la precipitación mensual en la España peninsular. Invest Geogr 26:41–58

Mishra AK, Singh VP (2010) A review of drought concepts. J Hydrol 391:202–216. doi:10.1016/j.jhydrol.2010.07.012

Moran MS, Clarke TR, Inque U, Vidal A (1994) Estimating crop water deficit using the relation between surface air temperature and spectral vegetation index. Remote Sens Environ 49:246–263

Moratiel R, Snyder RL, Durán JM, Tarquis AM (2011) Trends in climatic variables and future reference evapotranspiration in Duero Valley (Spain). Nat Hazards Earth Syst Sci 11:1795–1805

Nemani R, Pierce L, Running S, Goward S (1993) Developing satellite-derived estimates of surface moisture status. J Appl Meteorol 32:548–557

Nicholson SE, Tucker CJ, Ba MB (1998) Desertification, drought and surface vegetation: an example from the West African Sahel. Bull Am Meteorol Soc 79:815–829

Osborn TJ, Briffa KR, Tett SFB, Jones PD, Trigo RM (1999) Evaluation of the North Atlantic Oscillation as simulated by a climate model. Clim Dyn 15:685–702

Paolo AA, Rosa RD, Pereira LS (2012) Climate trends and behaviour of drought indices based on precipitation and evapotranspiration in Portugal. Nat Hazards Earth Syst Sci 12:1481–1491

Paredes D, Trigo RM, Garcia-Herrera R, Franco Trigo I (2006) Understanding precipitation changes in Iberia in early spring: weather typing and storm-tracking approaches. J Hydrometeorol 7:101–113

Parida BR, Oinam B, Patel NR, Sharma N, Kandwal R, Hazarika MK (2008) Land surface temperature variation in relation to vegetation type using MODIS satellite data in Gujarat state of India. Int J Remote Sens 29(14):4219–4235

Park S, Feddema JJ, Egbert SL (2004) Impacts of hydrologic soil properties on drought detection with MODIS thermal data. Remote Sens Environ 89:53–62

Patel NR, Barida BR, Venus V, Saha SK, Dadhwal VK (2011) Analysis of agricultural drought using vegetation temperature condition index from terra/MODIS satellite data. Environ Monit Assess 184(12):7153–7163. doi:10.1007/s10661-011-2487-7

Pereira LS, Paulo AA (2004) Droughts: concepts indices and prediction. In: Hamdy A, Trisorio-Liuzzi G (eds) Options méditerranéennes, series B, studies and research, water management for draught mitigation in the Mediterranean, vol 471. International Centre for Advanced Mediterranean Agronomic Studies, Bari, pp 13–144

Peters AJ, Reed BC, Eva MD, Havstad KM (1993) Satellite assessment of drought impact on native plant communities of southeastern New Mexico, U.S.A. J Arid Environ 24:305–319

Prihodko L, Goward SN (1997) Estimation of air temperature from remotely sensed surface observations. Remote Sens Environ 60:335–346

Rhee J, Im J, Carbone GC (2010) Monitoring agricultural drought for arid and humid regions using multi-sensor remote sensing data. Remote Sens Environ 114:2875–2887

Rodríguez-Puebla C, Nieto S (2010) Trends of precipitation over the Iberian Peninsula and the North Atlantic oscillation under climate change conditions. Int J Climatol 30(12):1807–1815

Rodríguez-Puebla C, Encinas AH, Nieto S, Garmendia J (1998) Spatial and temporal patterns of annual precipitation variability over the Iberian Peninsula. Int J Climatol 18:299–316

Rojas O, Vrieling A, Rembold F (2011) Assessing drought probability for agricultural areas in Africa with coarse resolution remote sensing imagery. Remote Sens Environ 115:343–352

Rouse JW, Hass RH, Schell JA, Deering DW (1974) Monitoring vegetation systems in the Great Plains with ERTS. In: Freden SC, Mercanti EP, Becker MA (eds) Proceedings of the 3rd Earth Resources Technology Satellite-1 symposium, Volume 1: Technical Presentations, p 309−317. Washington DC. NASA SP-351

Salinas-Zavala CA, Douglas AV, Diaz HF (2002) Inter-annual variability of NDVI in northwest Mexico. Associated climatic mechanisms and ecological implications. Remote Sens Environ 82:417–430

Sandholt I, Rasmussen K, Andersen J (2002) A simple interpretation of the surface temperature/vegetation index space for assessment of surface moisture status. Remote Sens Environ 79:213–224

Sannier CAD, Taylor JC (1998) Real-time vegetation monitoring with NOAA/AVHRR in Southern Africa for wildlife management and food security assessment. Int J Remote Sens 19:621–639

Santos J, Corte-Real J, Leite S (2007) Atmospheric large-scale dynamics during the 2004/2005 winter drought in Portugal. Int J Climatol 27:571–586. doi:10.1002/joc.1425

Santos J, Andrade C, Corte-Real J, Leite S (2009) The role of large-scale eddies in the occurrence of winter precipitation deficits in Portugal. Int J Climatol 29:1493–1507

Santos JF, Pulido-Calvo I, Portela MM (2010) Spatial and temporal variability of droughts in Portugal. Water Resour Res 46, W03503. doi:10.1029/2009WR008071

Singh RP, Roy S, Kogan F (2003) Vegetation and temperature condition indices from NOAA AVHRR data for drought monitoring over India. Int J Remote Sens 24(22):4393–4402

Solano R, Didan K, Jacobson A, Huete A (2010) MODIS Vegetation Index Users' Guide (MOD13 Series). Collection 5, Vegetation Index and Phenology Lab, University of Arizona (http://vip.arizona.edu) 1 – 42

Stisen S, Sandholt I, Nørgaard A, Fensholt R, Eklundh L (2007) Estimation of diurnal air temperature using MSG SEVIRI data in West Africa. Remote Sens Environ 110:262–274

Sun W, Wang PX, Zhang SY, Zhu DH, Liu JM, Chen JH, Yang HS (2008) Using the vegetation temperature condition index for time series drought occurrence monitoring in the Guanzhong Plain, PR China. Int J Remote Sens 29:5133–5144

Trigo RM, Osborn TJ, Corte-Real JM (2002) The North Atlantic Oscillation influence on Europe: climate impacts and associated physical mechanisms. Clim Res 20:9–17

Trigo RM, Pozo-Vázquez D, Osborn TJ, Castro-Díez Y, Gámiz-Fortis S, Esteban-Parra MJ (2004) North Atlantic Oscillation influence on precipitation, river flow and water resources in the Iberian Peninsula. Int J Climatol 24:925–944

USDA (1994) Major world crop areas and climatic profiles. World Agricultural Outlook Board. US Dep Agric Agric Handb 664:157–170

Vicente-Serrano SM (2006) Spatial and temporal analysis of droughts in the Iberian Peninsula (1910-2000)/Analyse spatio-temporelle des sécheresses dans la Péninsule Ibérique (1910-2000) Résume. Hydrol Sci J 51:83–97

Vicente-Serrano SM (2007) Evaluating the impact of drought using remote sensing in a Mediterranean semi-arid region. Nat Hazards 40:173–208

Vicente-Serrano SM, Heredia-Laclaustra A (2004) NAO influence on NDVI trends in the Iberian Peninsula (1982–2000). Int J Remote Sens 25(14):2871–2879

Vicente-Serrano SM, Trigo RM (2011) Introduction. In: Vicente-Serrano SM, Trigo RM (eds) Hydrological. Socioeconomic and Ecological Impacts of the North Atlantic Oscillation in the Mediterranean Region. Springer-Verlag, Berlin-Heidelberg-New York, pp 1–8. doi:10.1007/978-94-007-1372-7

Vicente-Serrano SM, Cuadrat JM, Romo A (2006) Aridity influence on vegetation patterns in the middle Ebro valley (Spain): evaluation by means of AVHRR images and climate interpolation techniques. J Arid Environ 66(2):353–375. doi:10.1016/j.jaridenv.2005.10.021

Wan Z (2007) MODIS Land Surface Temperature Products Users' Guide, Collection 5. ICESS. University of California, Santa Barbara, pp 1–30

Wan Z, Wang P, Li X (2004) Using MODIS Land Surface Temperature and Normalized Difference Vegetation Index products for monitoring drought in the Southern Great Plains, USA. Int J Remote Sens 25(1):61–72

Wang PX, Li X, Gong JY, Song C (2001) Vegetation temperature condition index and its application for drought monitoring. IEEE 2001 International Geoscience And Remote Sensing Symposium (IGARSS), 9-13 July 2001. The University of New South Wales, Sydney

Wilhite DA, Svoboda MD, Hayes MJ (2007) Understanding the complex impacts of drought: a key to enhancing drought mitigation and preparedness. Water Resour Manag 21(5):763–774. doi:10.1007/s11269-006-9076-5

Wu C, Chen JM, Desai AR, Hollinger DY, Arain MA, Margolis HA, Gough CM, Staebler RM (2012) Remote sensing of canopy light use efficiency in temperature and boreal forests of North America using MODIS imagery. Remote Sens Environ 118:60–72

Xoconostle-Cazares B, Ramirez-Ortega FA, Flores-Elenes L, Ruiz-Medrano R (2010) Drought tolerance in crop plants. Am J Plant Physiol 5(5):241–256. doi:10.3923/ajpp.2010.241.256